Available online www.jsaer.com

***Journal of Scientific and Engineering Research*, 2018, 5(9):221-232**

Research Article

ISSN: 2394-2630
CODEN(USA): JSERBR

Revisiting the Effect of the Corrosion Potential, the Matrix Resistivity and the Oxygen Availability on the Corrosion Rate of Steel Bars Embedded in Mortar

Gustavo S. Duffó[1,2,3,*], Enzo D. Gomez[1,3], Damián R. Vazquez[1,3]

[1]Comisión Nacional de Energía Atómica (CNEA), Gerencia Materiales, Depto. Corrosión. Av. Gral. Paz 1499, (1650) San Martín, Buenos Aires, Argentina
[2]Consejo Nacional de Investigaciones Científicas y Técnicas (CONICET), Buenos Aires, Argentina
[3]Universidad Nacional de San Martín (UNSAM), San Martín, Argentina

Abstract The parameters that control the corrosion process of steel bars embedded in concrete are the corrosion potential, the electrical resistivity and the oxygen availability. The objective of this work was to establish correlations between the corrosion rate and the mentioned parameters, to determine if the measurement of one of them, allows the estimation of the corrosion rate of the reinforcements. The parameters were measured in mortar specimens containing carbon steel and stainless steel bars. They were prepared with non-chloride addition and with chloride additions, in order to promote active corrosion; and were exposed for 18 months to different environmental conditions. The electrochemical parameters related to the state of the system were measured in a periodic basis. The results show the existence of very complex relationships between the measured parameters. It is concluded that it is not possible to predict the corrosion rate based on the measurement of the mentioned parameters.

Keywords reinforced concrete, corrosion, resistivity, oxygen availability

Introduction

It is well known that, in general, concrete provides a high degree of protection against corrosion of embedded reinforcing steel. The highly alkaline medium (pH>12.5) within the pores of the hardened cement matrix due to the hydration of the cement maintains the reinforcement in passive state. In this condition, the corrosion rate of the steel bars is very low due to the formation of a passive layer of iron oxides on the steel. Besides, the concrete cover also provides a physical protection because it acts as a barrier against access of aggressive species, such as carbon dioxide, and chloride ions. However, the initiation of the corrosion of the steel bars by the depassivation of the steel can occur because: (a) neutralization of the concrete by the atmospheric CO_2 that ingresses into the matrix, reducing the pH to about 9 and (b) localized breakdown of the passive layer (pitting corrosion) when the amount of chloride ions dissolved in the pore solution in contact with the reinforcing steel is higher than a threshold value [1-3].

The two main reactions involved in the corrosion of steel bars embedded in concrete are the oxidation of iron atoms, and the reduction of the oxygen molecules, according to the following hemi reactions:

$$Fe \rightarrow Fe^{2+} + 2\ e^- \quad [1]$$

$$O_2 + 4\ H_2O + 4\ e^- \rightarrow 4\ OH^- \quad [2]$$

In can be noted, from Eq. [2] than H_2O is one of the reactive necessary for the occurrence of the corrosion process.

The electrical resistivity of the matrix (ρ) takes into account the degree of water saturation (i.e. the amount of water in the pores), and the total ionic concentration of the pore solution. The concrete pore solution acts as an electrolyte with lower resistivity than the cement matrix, so the moisture content plays in fact a significant role

in determining the electrical properties of concrete [4,5]. This is why the electrical resistivity of concrete is one of the major factors in controlling the corrosion rate of the reinforcement. Several papers and reviews [6,11] deal with the effect of the electrical resistivity of the concrete on the corrosion rate of the steel, but a unique function between both parameters wasn't obtained.

On the other hand, as can be concluded from the eq. [2], the amount of oxygen that reaches the surface of the steel is another crucial parameter in the corrosion of reinforcing rebars. It is generally accepted that the oxygen reduction is the only cathodic reaction when steel corrodes embedded in concrete [12,13]. So, it is expected that corrosion rate of the steel rebars is primarily controlled by oxygen availability, that depends on the diffusion of dissolved oxygen through cover [4,14-17].

To sum up, to keep the corrosion process working, a continuous supply of oxygen is necessary to maintain the cathodic reaction and, together with the electrical resistance of the concrete, both parameters control the corrosion rate of the steel bars.

Another parameter related to the corrosion process is the corrosion potential (E_{corr}). Strictly speaking, the corrosion potential is the result of the corrosion process itself because this potential correspond to a potential value where the sum of all cathodic are equal to the sum of all anodic processes. The electrochemical potential characterises the state of a metal in its environment, and there is a standard that allows predicting the corrosion state of the rebars by the measurement of the corrosion potential [18].

The objective of the present work is to look for correlations between the corrosion rate (i_{corr}) and the electrochemical parameters frequently used to know the state of the reinforced concrete system: the corrosion potential (E_{corr}) , the electrical resistivity of the matrix (ρ) and the oxygen availability in terms of oxygen flow (i_{O2}), in order to determine if the measurement of one of them, allows the estimation of the corrosion rate of the reinforcements independently of the exposure conditions of the structure.

Experimental Technique

Experiments were performed on mortar prismatic specimens measuring 7×7×6 cm^3, containing four 6 mm diameter and 70 mm length smooth rods: two of them of SAE 1040 carbon steel and the other two of AISI 316 L stainless, as shown in Figure 1a. The carbon steel rods were used to measure the corrosion potential and the corrosion current density, while the stainless steel rods were used to measure the matrix resistivity as well as the oxygen flow through the matrix.

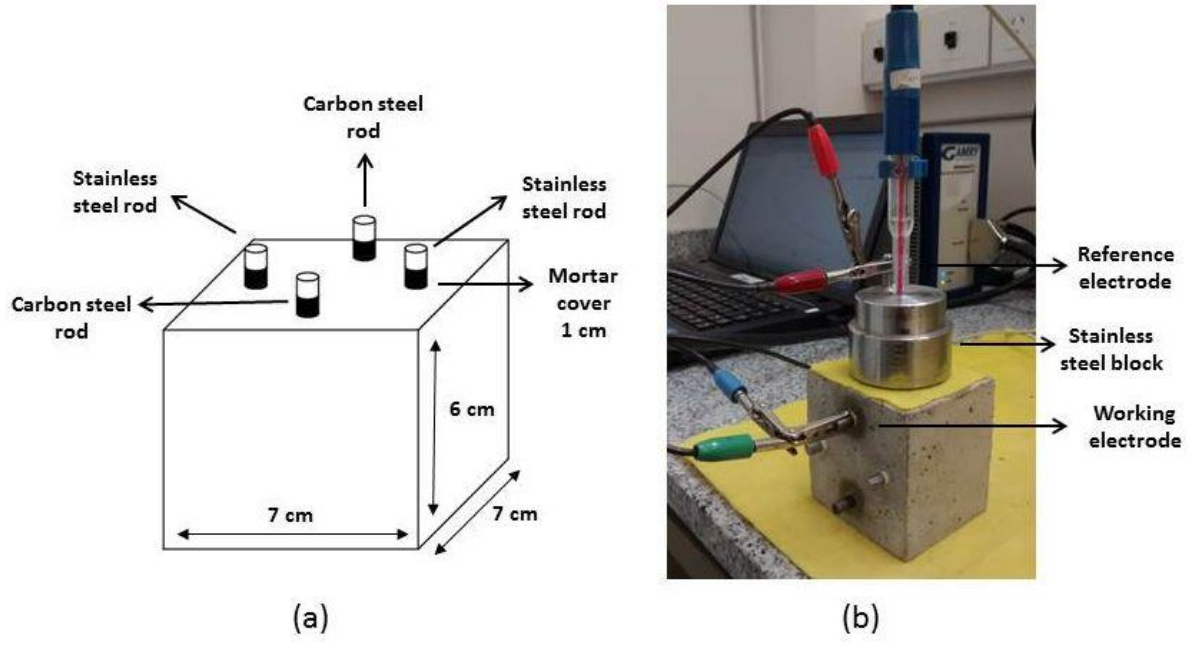

Figure 1: (a) Sketch of the mortar specimens used in the present work
(b) Experimental set-up used for the electrochemical measurements

All the rods were used in the as-received condition and degreased with ethyl acetate. These rods were embedded in mortar and the mortar-air interface was isolated with adhesive tape in order to avoid crevice corrosion due to differential aeration. The embedded ends of the rods were also covered with adhesive tape, to obtain an active surface area of 6.6 cm^2. The chemical composition of the carbon steel rods was (in wt.%): C, 0.39; Si, 0.30; Mn, 0.66; P, 0.007; S, 0.005; Cr, 0.04; Ni, 0.02; Mo, <0.003 and Fe, balance. The chemical composition of the stainless steel rods was: Cr 17.4; Ni 12.1; C 0.023; Mn 1.7; Si 0.4; P 0.029; Si 0.008; Mo 2.44 and Fe balance

Mortar specimens were prepared with a cement/sand/water ratio of 1/3/0.6. The cement used was normal portland cement (CPN 40 ARS, Loma Negra™) and its chemical composition is shown in Table 1.

Table 1: Chemical composition of the cement used in the present work

Chemical composition	**(%)**
Loss by calcination (%)	0.87
Insoluble residue (%)	2.65
Sulphur trioxide (SO3) (%)	1.73
Magnesium Oxide (MgO) (%)	1.60
Silicon dioxide (SiO_2) (%)	19.86
Ferric Oxide (Fe_2O_3) (%)	4.19
Aluminium Oxide (Al_2O_3) (%)	4.11
Calcium Oxide (CaO) (%)	63.82
Sodium Oxide (Na_2O) (%)	0.01
Potassium Oxide (K_2O) (%)	0.93
Chloride (Cl^-) (%)	0.03

Eight mortar specimens with non-chloride additions (NC) and six specimens containing 5% chloride/cement added as NaCl chloride (C) were prepared according to ASTM C-305 Standard [19]. The mortar was cast in metallic moulds and after curing for 24 h, the mortar blocks were taken from the moulds and kept at 98% RH at room temperature for 28 days (moist curing). After the moist curing, the specimens were exposed to different environmental condition: two NC and two C specimens in a 98% relative humidity chamber (condition H98); two NC and two C specimens in laboratory environment with a relative humidity between 55 and 85% (condition HR), two NC and two C specimens immersed in a 3.3% chloride aqueous solution prepared with NaCl analytical grade reagent (condition CS) and two NC specimens immersed in deionized water (condition DW)

To determine the electrochemical parameters, a Gamry Ref 600 Potentiostat-Galvanostat was used in all cases. The electrical resistivity of the mortar (ρ) was determined from the resistance measurements of the matrix. This was performed by applying a sinusoidal signal (ΔV=10mV, ν=10 kHz) between one of the stainless steel rods (acting as working electrode) and the reference electrode, using a stainless steel block as a counter electrode (Figure 1b), and computing the value of the resistance as the real part of the impedance obtained. In order to determine the electrical resistivity from the resistance measurement, a calibration with KCl aqueous solutions (ranging from $1x10^{-5}$ to 1M) of known resistivity was performed [13].

To determine the corrosion rate of the carbon steel bars, the galvanostatic pulse technique was applied [20]. The configuration used is shown in Figure 1b, where the working electrode is the carbon steel rod. The corrosion potential of the carbon steel rods was measured until a quasi-constant value was reached and then, a galvanostatic pulse of 120 seconds was applied at a current density (I_{app}) selected in order to avoid polarization of the steel rods higher than 30 mV. From the $\Delta E - I_{app}$ behaviour, the polarization resistance was obtained in the usual way [20], and then, the corrosion current density (i_{corr}) was computed [21].

Finally, the determination of the oxygen flow was based on the assumption that when a negative potential (within certain limits) is applied to an inert electrode embedded in concrete, the only cathodic reaction taking place is the oxygen reduction at the electrode surface [12,13]. In the present work, the oxygen flow was determined with the configuration shown in Figure 1b. The circulating current density (i_{O2}) after polarizing one of the stainless steel rods for 300 sec at -1.050 V_{SCE}, using the stainless steel block as a counter electrode was

taken as the oxygen flow. The value of the applied potential was selected after calibrating the technique for all the environmental condition studied.

All the measurements were done in a regular basis during 1.5 years. The distribution of the specimens in the different environment lets to obtain results by quadruplicate. Repetitive results were obtained in all cases and so, in the description of the results, only one result for condition is shown.

Results and Discussion

Figure 2 shows the evolution of the corrosion potential as a function of time during 550 days, for specimens with non-chloride addition. The limits given by the ASTM C 876-04 [18] standard are included in order to evaluate the meaning of the results. It can be seen that specimens exposed to the laboratory environment (HR) show the higher corrosion potential and, according to the standard, the lower corrosion probability. On the other hand, specimens exposed to a chloride aqueous solution, show the lower corrosion potential and hence, according to the standard, the higher corrosion probability. The specimens exposed to a 98% relative humidity as well as immersed in deionized water show results in the uncertain corrosion activity zone.

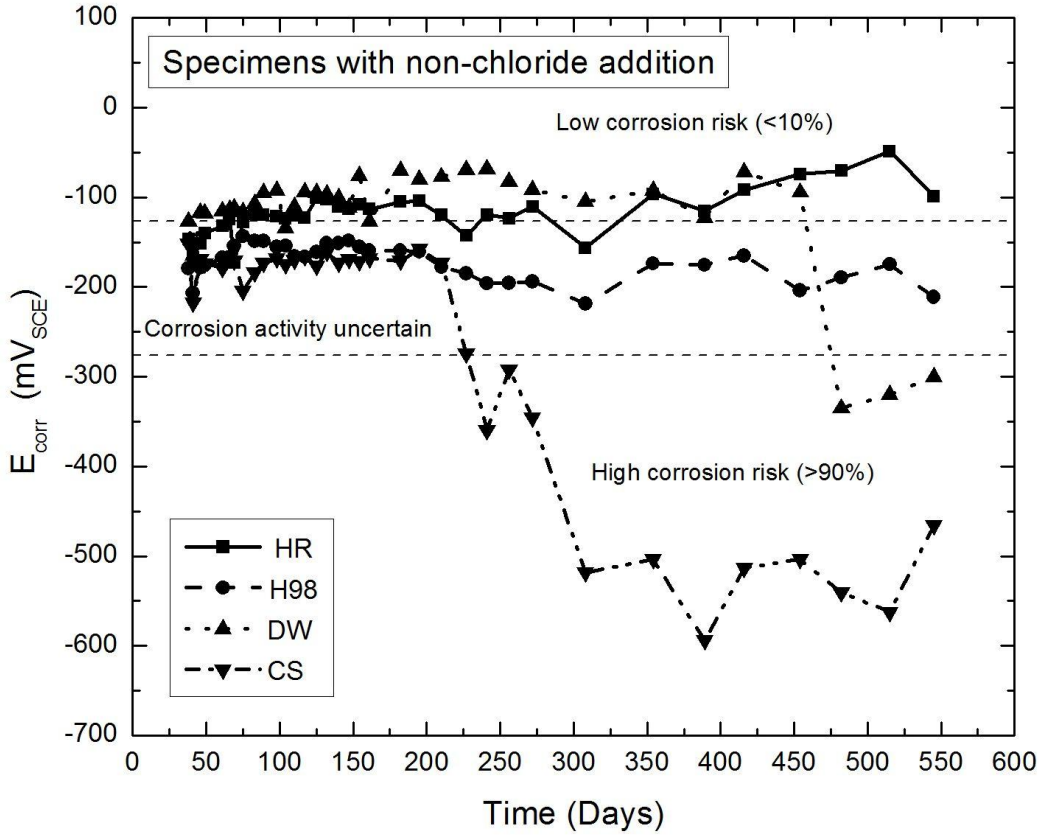

Figure 2: Evolution of the corrosion potential as a function of time, for specimens with non-chloride addition. The limits given by the ASTM C 876-04 standard [18] are included.

In Figure 3, the corrosion potentials measured during 550 days in specimens with chloride addition are shown. In all cases, values lies inside the high corrosion risk zone, according to the ASTM C 876-04 standard [18].

Figure 4 shows the corrosion current density values measured on specimens with non-chloride addition. The limits suggested by McCarter and Vennesland [22] are included to evaluate the results.

It can be observed that specimens exposed to a laboratory environment and 98% relative humidity show the lower corrosion current density that lies in the negligible corrosion rate zone. On the other hand, specimen immersed in aqueous solutions (deionized water and aqueous chloride solution) show higher corrosion current densities that belong to a moderate or high corrosion rate.

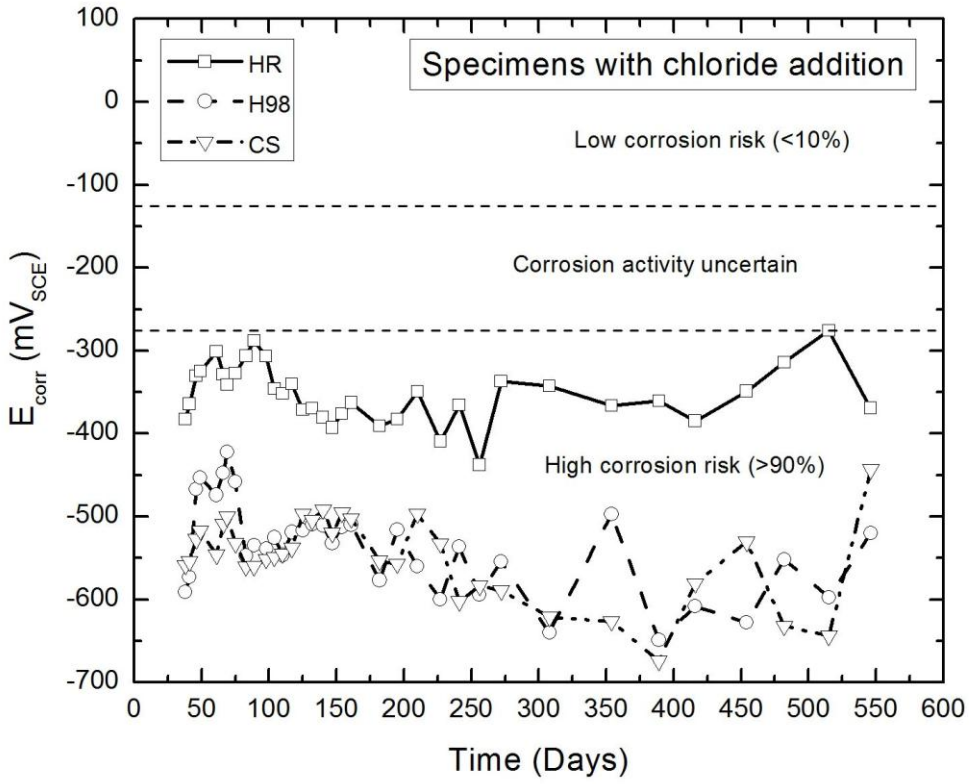

Figure 3: Evolution of the corrosion potential as a function of time, for specimens with chloride addition. The limits given by the ASTM C 876-04 standard [18] are included.

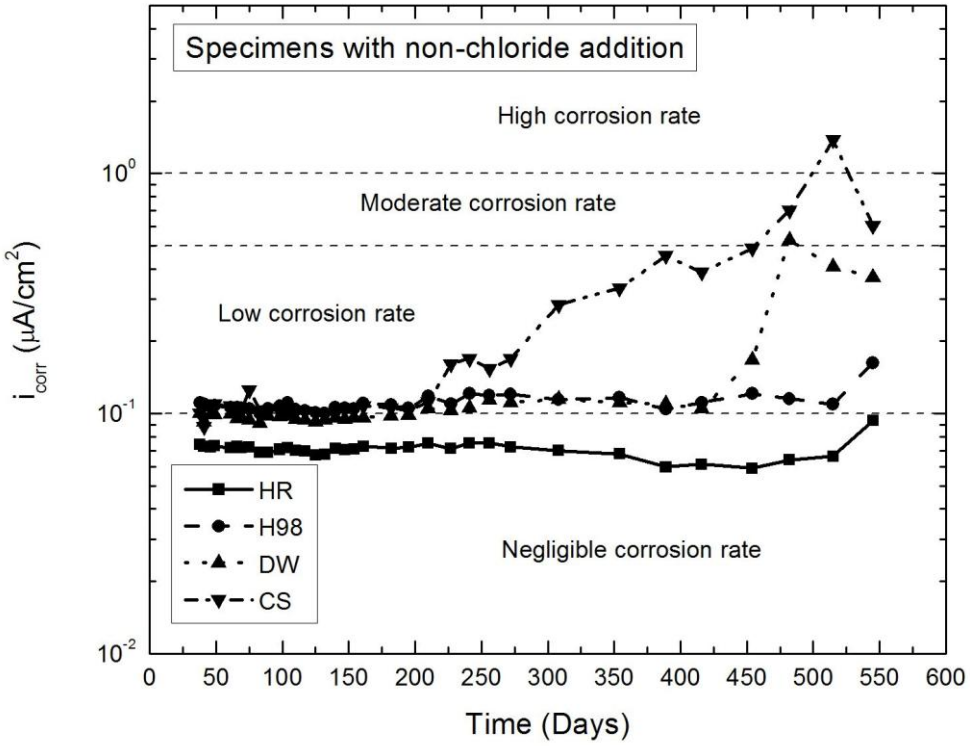

Figure 4: Evolution of the corrosion current density as a function of time, for specimens with non-chloride addition The corrosion rate limits suggested in [22] are included.

In Figure 5, the corrosion current density measured during 550 days on specimen with chloride addition is shown. The results lie in the low and moderate corrosion rate zone.

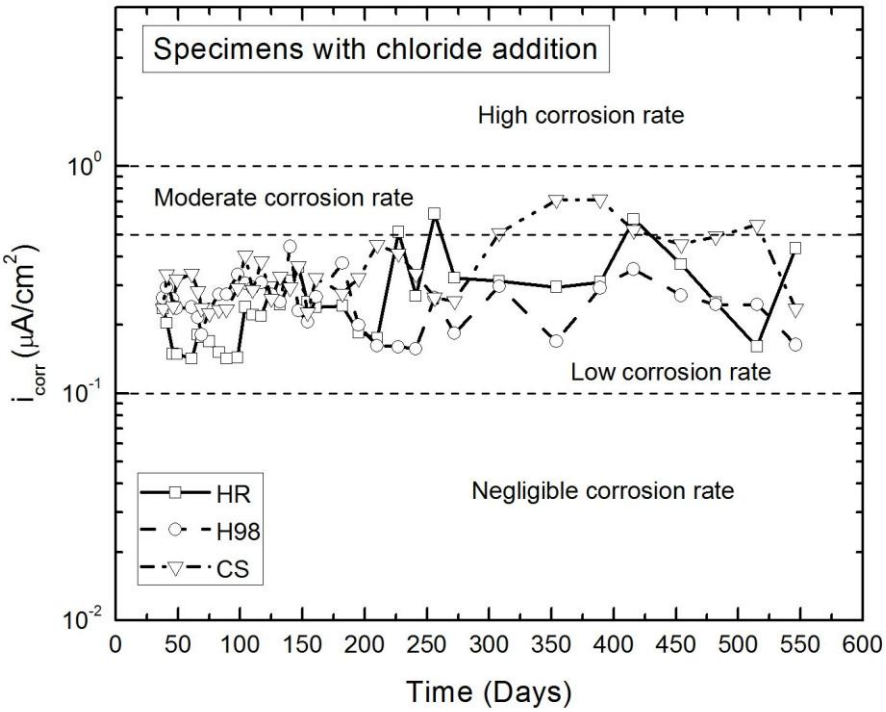

Figure 5: Evolution of the corrosion current density as a function of time, for specimens with chloride addition. The corrosion rate limits suggested in [22] are included

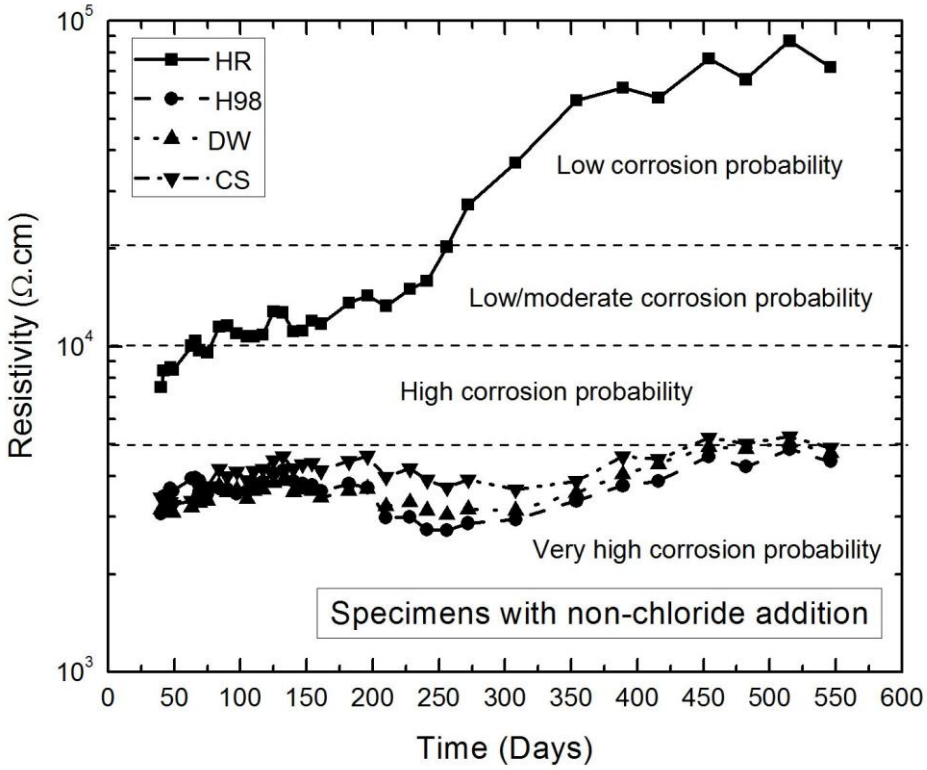

Figure 6: Evolution of the electrical resistivity as a function of time, for specimens with non-chloride addition. The limits suggested in [22] are included

Figure 6 shows the evolution of the electrical resistivity of the mortar matrix as a function of time, for specimens with non-chloride addition. The limits of the corrosion probability as a function of the electrical resistivity suggested by McCarter and Vennesland [22] are included for the sake of comparison. It can be seen that, for specimens exposed to laboratory environment, the electrical resistivity continuously increases with the exposure time, being this fact an indication of the continuous concrete hydration process. However, specimens exposed to a humid environment (relative humidity 98%) as well as immersed in aqueous solution, only show a small increase with time, reaching a value close to 5000 ohm.cm after 550 days of exposure.

The results obtained for specimen with chloride addition (Figure 7) are similar to those reported for specimens with non-chloride addition, for a qualitative point of view. However, the values obtained in this case are lower because of the effect of the chloride ion that increases the conductivity of the pore solution and hence, decreases the resistivity. Only the specimens exposed to laboratory environment with non-chloride addition show results that lie in the low corrosion probability zone, while in the other cases, the results lie in the high or very high corrosion probability zone.

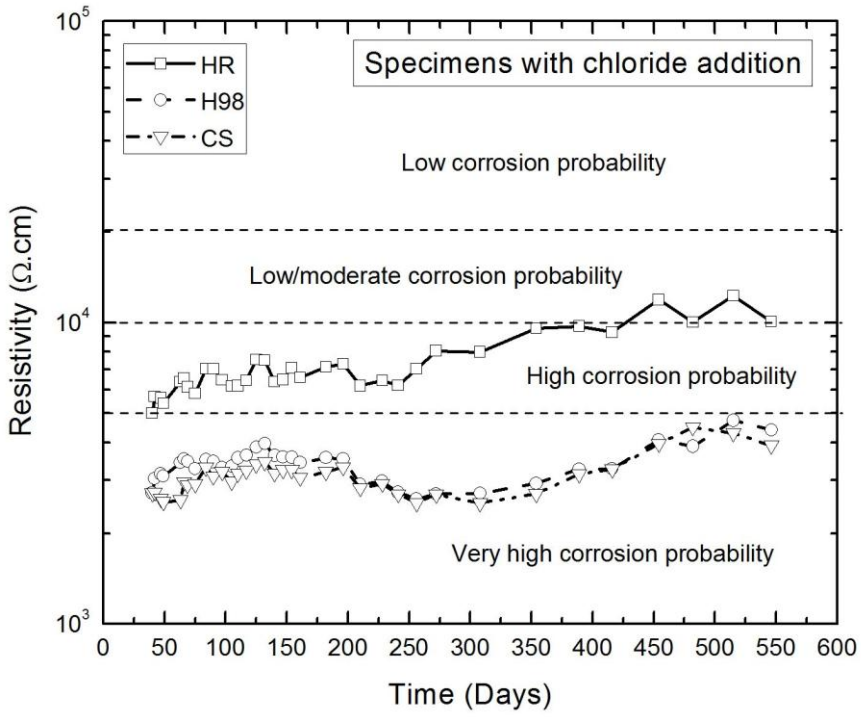

Figure 7: Evolution of the electrical resistivity as a function of time, for specimens with chloride addition. The limits suggested in [22] are included.

Figures 8 and 9 show the limiting current density associated with the oxygen flow as a function of time, for specimens with non-chloride and with chloride addition, respectively. For specimens exposed to laboratory environment (with non-chloride and with chloride addition), this parameter decreases almost exponentially as a function of time, while for the other conditions, the oxygen flow remains almost constant during the duration of test.

Figure 10 shows the results corresponding to the relationship between i_{corr} and E_{corr} obtained for all the conditions studied in the present work during 1.5 years measurement. The figure includes E_{corr} ranges where the ASTM C 876-04 standard [18] predicts different corrosion probabilities. The figure also includes i_{corr} ranges that, according to some recommendations [22-24], belong to different conditions of the steel rebars concerning its susceptibility to corrosion. In one case, the recommendation only mentions the different states of the steel rebar taking into account the presence or not of a passive state [23]. On the other hand, the other recommendation puts the focus on the dangerousness of the corrosive attack [22,24].

It seems to be that a linear relationship could be obtained from the data, but the error in predicting i_{corr} from a E_{corr} measurement is very large. For instance, for a E_{corr} value of -0.4 V_{SCE}, i_{corr} from 0.1 to 2 μA/cm^2 could be predicted. Even more, from Figure 10, although ASTM C 876-04 standard [18] predicts corrosion probabilities higher than 90% for corrosion potentials lower than -0.280 V_{SCE}, less than this percentage of the results lie in the active state region according to the i_{corr} values [23].

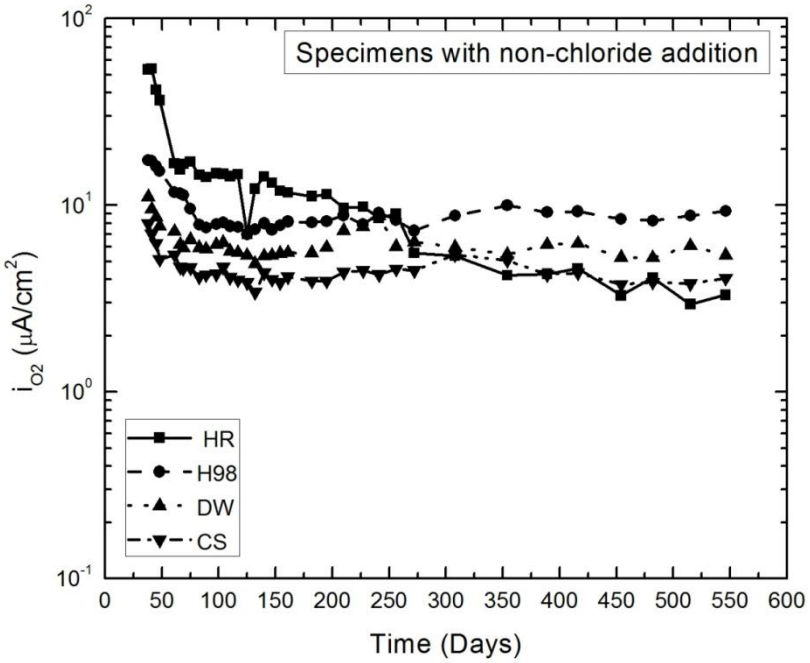

Figure 8: Evolution of the oxygen flow (measured as current density) as a function of time, for specimens with non-chloride addition

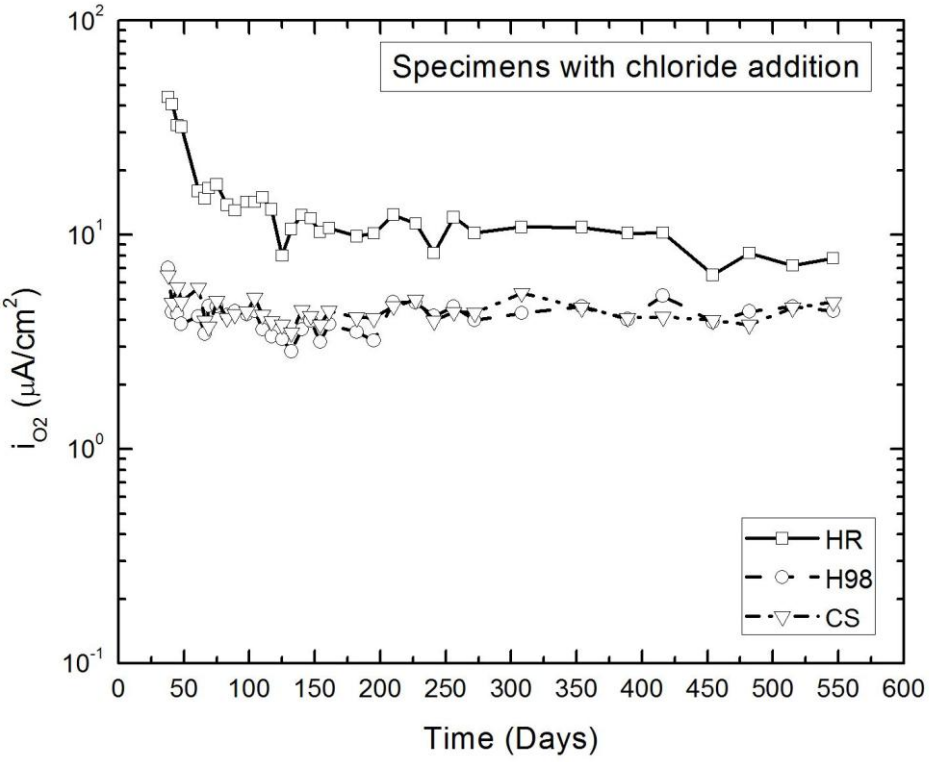

Figure 9: Evolution of the oxygen flow (measured as current density) as a function of time, for specimens with chloride addition.

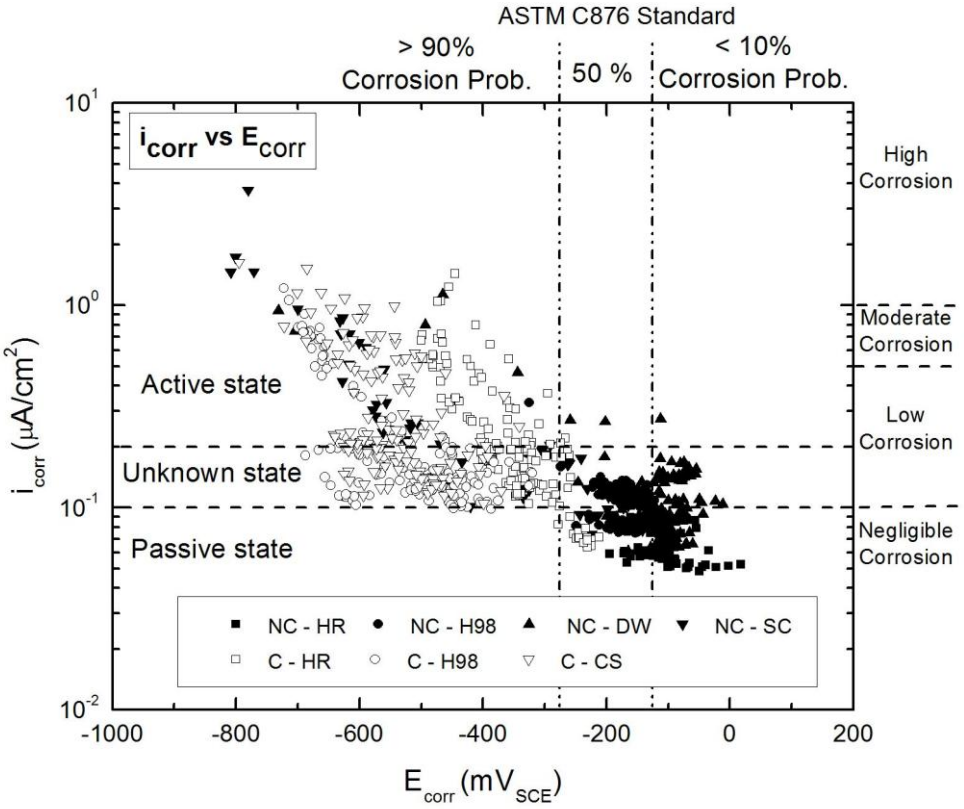

Figure 10: Relationship between corrosion current density and corrosion potential for all the conditions studied. Data ranges suggested by ASTM C 876-04 [18] and recommendations [22-24] are also included.

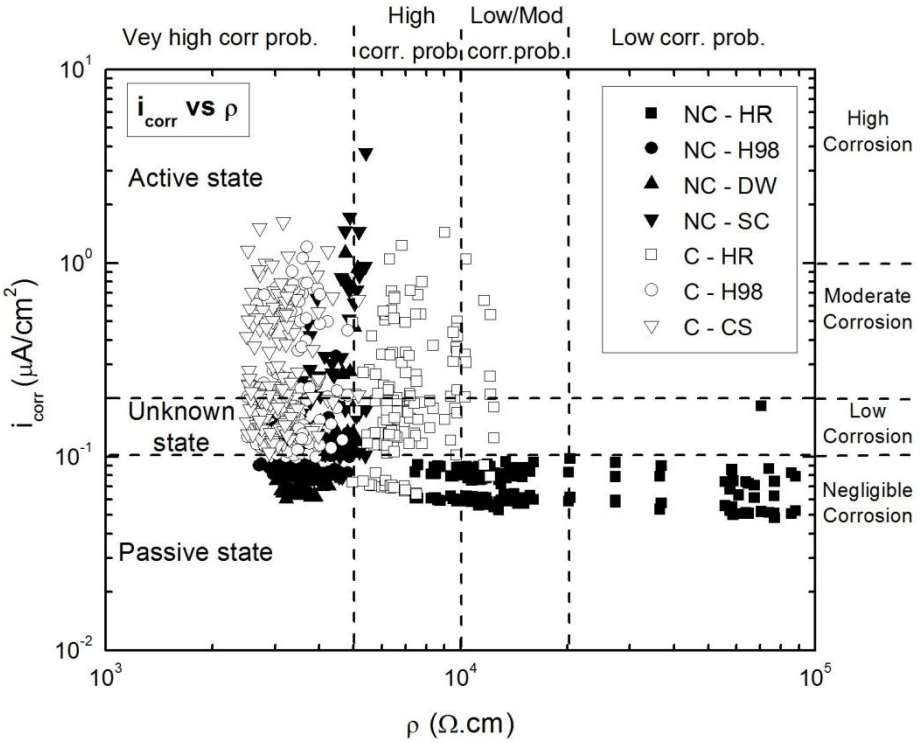

Figure 11: Relationship between corrosion current density and electrical resistivity of the matrix for all the conditions studied. Data range suggested in [22-24] are included.

Figure 11 shows the results corresponding to the relationship between i_{corr} and ρ obtained for all the conditions studied in the present work during 1.5 years (550 days). The figure also includes the i_{corr} dangerousness ranges suggested by the literature [22-24]. The general behaviour is similar to those reported in previous publications: the higher the ρ, the lower the i_{corr} [6-11]. However, it can be seen that, in spite of the some attempts reported in the literature to obtain a relationship between i_{corr} and ρ, from Figure 11 it is concluded that it not possible to predict with certainty the value of i_{corr} from the ρ measurements. The knowledge of ρ only lets obtain a range of i_{corr} values, and in this case, the higher the ρ, the shorter the i_{corr} range predicted. So, only the measurement of larger ρ values (>3.10^4 Ω.cm) let assure that the i_{corr} will be in the passive state region (or negligible corrosion rate.

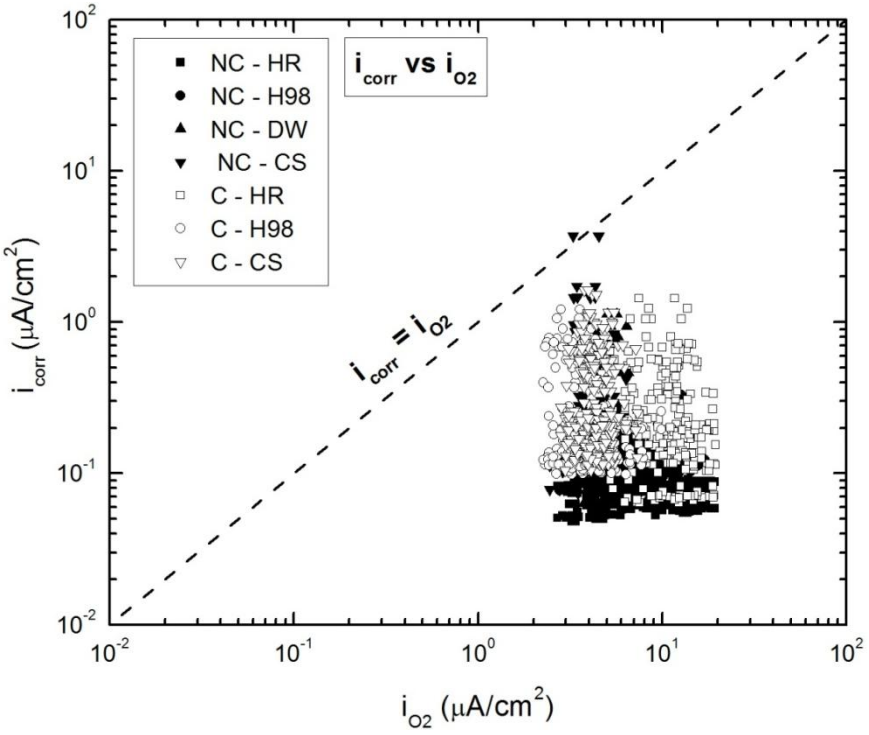

Figure 12: Relationship between corrosion current density and oxygen flow for all the conditions studied

Figure 12 shows the results corresponding to the relationship between i_{corr} and i_{O2} obtained for all the conditions studied in the present work during 1.5 years. It is important to remark that the i_{O2} values presented correspond to the limiting cathodic current density measured for each experimental condition. From Figure 12 it should be noted that all data accumulate in a small region and that, except from a couple of data, the i_{corr} values are always lower than the i_{O2} values; i.e. all data are below the straight line $i_{corr} = i_{O2}$. This led to induce that the anodic branch of the hemi reaction belonging to the iron oxidation (Eq [1]) does not crosses the cathodic branch of the oxygen reduction hemi reaction (Eq [2]) in its limiting current density region. Instead of that, the oxygen reaction could be in its charge transfer controlled zone. This topic deserves further studies. From the results shown in Figure 12, it can be concluded that the simple measurement of the i_{o2} does not provide a unique value of i_{corr}.

Finally, taken into account that i_{O2} account for the rate of the reaction shown in Eq [2], and that the reaction involves the presence of water (whose contents, among other factors, determine the ρ value), it is expected that some relationship between both parameters should appears. Figure 13 shows the results obtained for i_{O2} as a function of ρ. In spite of the previous predictions, not correlation was obtained. Filtering the information shown in Figure 13 and taking into account only the results obtained for the HR condition (with and without chloride additions), an almost linear relationship was obtained: the higher the ρ value, the lower the i_{O2} value. This is due to the fact that the higher ρ values the lower the water content in the pores, and hence, Eq. [2] is hindered. The results for the other conditions accumulate in a narrow region of ρ values, while i_{O2} changes one order of magnitude.

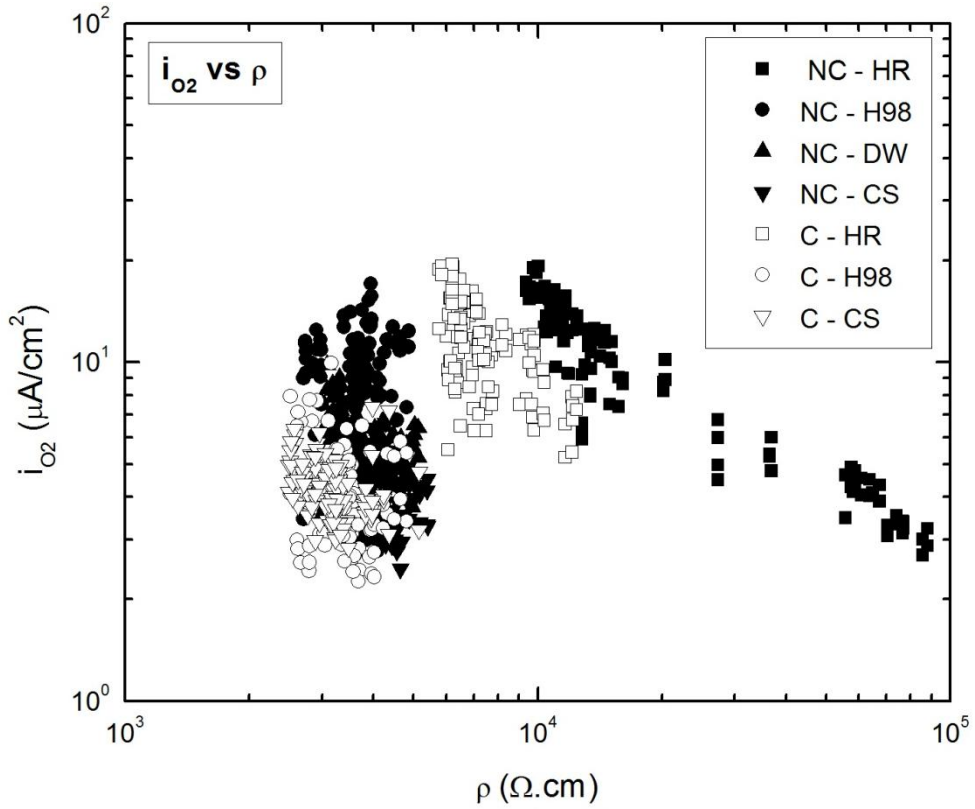

Figure 13: Relationship between oxygen flow and matrix electrical resistivity for all the conditions studied

Conclusions

- It is not possible to establish correlations to predict i_{corr} values based on other parameters such as E_{corr}, ρ or i_{O2}.
- In spite of the standard ASTM C-876-04 recommendations, the condition of a reinforcing bar cannot be unambiguously established by a single measurement of E_{corr}
- In systems exposed to laboratory environment (HR), the matrix parameters (i_{O2} and ρ) are inversely proportional.
- The only measurement that gives the real state of a reinforcing bar is i_{corr} and its measurements cannot be replaced for the measurement of other parameters of the system.

Acknowledgments

The financial support of the CONICET (Consejo Nacional de Investigaciones Científicas y Técnicas), and of the FONCYT, Secretaría para la Tecnología, la Ciencia y la Innovación Productiva, Argentina, is acknowledged.

References

[1]. Broomfield J.P. (1997). *Corrosion of Steel in Concrete. Understanding, investigation and repair*. E & FN SPON, London and New York, 10-20.

[2]. Bentur A., Diamond S., Berke N.S. (1997). *Steel Corrosion in Concrete: Fundamentals and Civil Engineering Practise*. Taylor & Francis, London, 24-58.

[3]. Pedeferri P., Polder B., Bertolini L., Elsener B. (2004). *Corrosion of Steel in Concrete: Prevention, Diagnosis, Repair*. Wiley-VCH, Weinheim, 69-76.

[4]. Hunkeler, F. (2005). *Corrosion in reinforced concrete: processes and mechanisms*, in *Corrosion in reinforced concrete structures*. Böhni, H., Ed. Ed. Woodhead Publishing Ltd, Cambridge, 1-45.

[5]. Lopez, W., Gonzalez, J. (1983). Influence of the degree of pore saturation on the resistivity of concrete and the corrosion rate of steel reinforcement. *Cem. Concr. Res.*, 23: 368-376.

[6]. Morris, W., Vico, A., Vazquez, M., de Sanchez, S.M. (2002). Corrosion of reinforcing steel by means of concrete resistivity measurements. *Corros. Sci.*, 44: 81-99.
[7]. Morris, W., Vico, A., Vázquez, M. (2004). Chloride induced corrosion of reinforcing steel evaluated by concrete resistivity measurements. *Electrochim. Acta.*, 49: 4447-4453.
[8]. Glass, G.K., Page, C.L., Short, N.R. (1991). Factors affecting the corrosion rate of steel in carbonated mortars. *Corros. Sci.*, 32: 1283-1294.
[9]. Enevoldsen, J.N., Hansson, C.M. (1994). The influence of internal relative humidity on the rate of corrosion of steel embedded in concrete and mortar. *Cem. Concr. Res.*, 24: 1373-1382.
[10]. Alonso, C., Andrade, C., González, J.A. (1988). Relation between resistivity and corrosion rate of reinforcements in carbonated mortar made with several cement types. *Cem. Concr. Res.*, 18: 687-698.
[11]. Saleem, M., Shameem, M., Hussain, S.E., Maslehuddin, M. (1996). Effect of moisture, chloride and sulphate contamination on the electrical resistivity of portland cement concrete. *Constr. Build. Mater.*, 10: 209-214.
[12]. Gjorv O.E., Vennesland, Ø, El-Busaidy, A.H.S. (1986). Diffusion of dissolved oxygen through concrete. *Mater. Performance*, 25: 39-44.
[13]. Duffó, G.S., Farina, S.B. (2009). Development of an embeddable sensor to monitor the corrosion process of new and existing reinforced concrete structures. *Constr. Build. Mater.*, 23: 2746-2751.
[14]. Andrade, C., Alonso, C., García, A.M. (1990). Oxygen availability in the corrosion of reinforcements. *Adv. Cem. Res.*, 3: 127-132.
[15]. Hansson, C.M. (1993). Oxygen diffusion through portland cement mortars. *Corros. Sci.*, 35: 1551-1556.
[16]. Raupach, M. (1996). Investigations on the influence of oxygen on corrosion of steel in concrete - Part l. *Mater. Struct.*, 29: 174–184.
[17]. Raupach, M. (1996). Investigations on the influence of oxygen on corrosion of steel in concrete - Part II. *Mater. Struct.*, 29: 226-232.
[18]. American Society of Testing and Materials (ASTM) C 876-04 (2004). Test method for half-cell potentials of uncoated reinforcing steel in concrete. West Conshohocken, PA.
[19]. American Society of Testing and Materials (ASTM) C305 (2014). Standard practice for mechanical mixing of hidraulic cement pastes and mortars of plastic consistency, West Conshohocken, PA.
[20]. Sathiyanarayanan, S., Natarajan, P., Saravanan, K., Srinivasan, S., Venkatachari, G. (2006). Corrosion monitoring of steel in concrete by galvanostatic pulse technique. *Cem. Concr. Compos.*, 28: 630-637.
[21]. Andrade C, Gonzalez J.A. (1978). Quantitative measurements of corrosion rate of reinforcing steels embedded in concrete using polarization resistance measurements. *Werkst Korros.*, 29: 515-519.
[22]. McCarter, W.J., Vennesland, Ø. (2004). Sensor systems for use in reinforced concrete structures. *Constr. Build. Mater.*, 18: 351-358.
[23]. Andrade, C., Alonso, C. (2001). On-site measurements of corrosion rate of reinforcements. *Constr. Build. Mater.*, 15: 141-145.
[24]. Andrade, C., Alonso, C., Gulikers, J., Polder, R, Cigna, R., Vennesland, O., Salta, M., Raharinaivo, A., Elsener, B. (2004). Test methods for on-site corrosion rate measurement of steel reinforcement in concrete by means of the polarization resistance method. *Mater. Struct./ Matériaux Constr.*, 37: 623-643.